Real-Time Characterization of Biogeochemical Reduction of Cr(VI) on Basalt Surfaces by SR-FTIR Imaging

HOI-YING N. HOLMAN
DALE L. PERRY

Center for Environmental Biotechnology
E. O. Lawrence Berkeley National Laboratory
Berkeley, California, USA

MICHAEL C. MARTIN
GERALDINE M. LAMBLE
WAYNE R. McKINNEY

Advanced Light Source Division
E. O. Lawrence Berkeley National Laboratory
Berkeley, California, USA

JENNIE C. HUNTER-CEVERA

Center for Environmental Biotechnology
E. O. Lawrence Berkeley National Laboratory
Berkeley, California, USA

Synchrotron radiation-based (SR) Fourier-transform infrared (FTIR) spectromicroscopy in the mid-infrared region is a surface analytical technique that can provide direct insights into the localization and real-time mechanisms for the reduction of the $(CrO_4)^{2-}$ chromate [Cr(VI)] species on surfaces of geologic materials. Time-resolved SR-FTIR spectra indicate that, in the presence of endoliths (mineral-inhabiting microorganisms), microbial reduction of Cr(VI) to Cr(III) compounds on basaltic mineral surfaces is the key mechanism of Cr(VI) transformation. It proceeds in at least a two-step reaction with Cr(V) compounds as possible intermediate products, with the reduction of Cr(VI) increasing during the concomitant biodegradation of a dilute organic vapor (toluene). Analyses of spatially resolved SR-FTIR spectra show that the maximum reduction of Cr(VI) to Cr(III) compounds occurs on surfaces densely populated by microorganisms. The oxidation state of Cr(III) compounds was confirmed by micro-x-ray absorption fine-structure spectroscopy. Both the time- and space-resolved SR-FTIR spectra show that in the absence of endoliths, Cr(VI) reduction is insignificant. With this effort, the potential use of SR-FTIR spectromicroscopy in providing mechanistic information of reduction of Cr(VI) has been demonstrated. This method can now be expanded to examine other IR-amenable microbial/chemical contaminant systems.

Keywords Cr(VI), endolithic microorganisms, FTIR, infrared spectroscopy, x-ray absorption spectroscopy

Received 21 June 1999; accepted 29 June 1999.

We thank Drs. Terry C. Hazen, Tamas Torok, and Arthur Robinson for reviewing the manuscript, and Dr. Tamas Torok for conducting the FAME analysis. The work was supported by the Office of Science of the United States Department of Energy under Contract No. DE-AC03-76SF00098 and by the U.S. Army Corps of Engineers of the Department of Defense under Contract No. DAC39-95-2-0005.

Address correspondence to Dr. Hoi-Ying N. Holman, Center for Environmental Biotechnology, E.O. Lawrence Berkeley National Laboratory, Berkeley, CA 94720, USA. E-mail: hyholman@ lbl.gov

Geomicrobiology Journal, 16:307–324, 1999
Copyright © 1999 Taylor & Francis
0149-0451/99 $12.00 + .00

Designing effective strategies to immobilize and detoxify metal ions of high-oxidation states in geologic materials requires an accurate characterization and fundamental understanding of the nature of biogeochemical reactions at metal ion/geologic material interfaces. This surface biogeochemistry can be highly variable at a microscopic level, which arises from the small-scale (ranging from 1 μm to hundreds of micrometers) surface heterogeneity involving the distributions of clusters of endoliths (mineral-inhabiting microorganisms), reactive molecules of metal oxides, and/or organic molecules. The methodology commonly used to study this heterogeneous biogeochemical phenomenon is a combined microscopic imaging and x-ray spectromicroscopy technique. This includes, for example, x-ray absorption fine-structure (XAFS) spectroscopy (Peterson et al. 1997; Cheah et al. 1998; Conradson 1998), x-ray fluorescence (XRF) spectroscopy (Kaplan et al. 1994), and x-ray photoelectron spectroscopy (XPS) (Perry et al. 1990; Biino et al. 1998; Fiedor et al. 1998). However, the irradiation intensity associated with x-ray spectromicroscopy techniques can damage the endoliths, and thus has defeated the use of x-ray spectromicroscopy techniques for studying the biogeochemical reactions as they are occurring at the metal ions/endolith/mineral interfaces.

In this paper we describe a study that explored and used a nondestructive method to complement the above-mentioned x-ray absorption surface chemistry techniques. The method uses synchrotron radiation-based (SR) Fourier-transform infrared (FTIR) spectromicroscopy to study real-time biogeochemical reactions at the metal ion/endolith/mineral interfaces. SR-FTIR spectromicroscopy is used because this sensitive analytical technique has been proven capable of providing direct molecular information on surface compositions at a (diffraction-limited) spatial resolution of 10 μm or better. For example, Bantignies et al. (1995) demonstrated that SR-FTIR spectromicroscopy could be used to analyze the composition of clay mineral surfaces. Guilhaumou et al. (1998) successfully mapped fluid inclusions and volatilization in geologic materials, using similar instrumentation. Recently Jamin et al. (1998) showed that the instrumentation sensitivity is sufficient to map the distribution of functional groups of biomolecules such as proteins, lipids, and nucleic acids with a spatial resolution of a few micrometers.

To explore and demonstrate the efficacy of SR-FTIR spectromicroscopy as a promising tool for elucidating the mechanisms and the pathways of metal transformations as the reactions are happening at the metal ions/endolith/mineral interfaces, we used the method to investigate the biogeochemical reduction of the chromate ion [Cr(VI)] in geologic materials. This contaminant/endolith/mineral system was selected because it is one system for which real-time interfacial information of the Cr(VI) transformation draws intense interest. Cr(VI) is a widespread, highly mobile, and toxic contaminant that enters the environment through various industrial processes. When in the oxidized hexavalent form, the chromium readily crosses cell membranes mainly via the sulfate $(SO_4)^{2-}$ active transport system (Ehrlich 1990), becomes toxic to many ecological receptors, and is carcinogenic to mammals (Ohtake and Silver 1994; Snow 1991). When in the reduced trivalent form, the chromium tends to form relatively insoluble compounds that often cannot cross cell membranes and thus become substantially less harmful to the same biological systems (Nieboer and Jusys 1988). Recent studies have confirmed that certain species of bacteria (Wang and Shen 1995; Turick et al. 1996; Lovley and Coates 1997; Silver 1998), molecules of mixed mineral oxides [such as Fe(II), Fe(III), Mn(II), Mn(III), and Mn(IV)], and many small organic compounds can catalyze the reduction of Cr(VI) to Cr(III) (Bidoglio et al. 1993; Deng and Stone 1996; Guo et al. 1997). This has stimulated keen interest in the exploration of the biogeochemical reduction of the Cr(VI) metal ions in geologic materials (e.g., Losi et al. 1994; Shen et al. 1996; Ahmann, 1997) to obtain insights into the selection and improvement of remediation strategies to immobilize and detoxify Cr(VI) .

The SR-FTIR spectromicroscopy experiments of the selected biogeochemical phenomenon were first conducted on surfaces of a model mineral phase with and without the concomitant biodegradation of a model organic co-contaminant, and then on surfaces of geologic samples from a contaminated site with the model organic co-contaminant. Magnetite was selected as the model mineral phase because it is a ubiquitous component of geologic materials (Kostka and Nealson 1995) and is extremely efficient in the adsorption of bacterial cells (Wong and Fung 1997). *Arthrobacter oxydans*, a widespread Gram-positive endolithic bacterium found in our geologic samples (see below), was used to model Cr(VI)-tolerant and -reducing bacteria. Toluene vapor was selected as a model organic co-contaminant, because this type of small aromatic hydrocarbon is commonly found as a co-contaminant in many Cr-contaminated sites (Shen et al. 1996). At the end of the SR-FTIR spectromicroscopy study, the final spatial distribution of chromium on surfaces of geologic samples was validated by micro-x-ray fluorescence (μ-XRF) spectroscopy. The oxidation state of detected chromium was validated by micro-x-ray absorption fine-structure (μ-XAFS) spectroscopy. Our results have not only demonstrated the usefulness of the SR-FTIR technique but also revealed the possible pathway of Cr(VI) reduction and the strong correlation between Cr(VI) reduction and areas of mineral surfaces where endoliths are prevalent.

Materials and Methods

Chemicals and Chemical Model Compounds

All experimental chemicals were ACS-reagent grade and purchased from Aldrich (USA). Chromium(III) model compounds used for SR-FTIR spectral calibration were chromium(III) acetate monohydrate, $Cr(C_2H_3O_2)_3 \cdot H_2O$, and chromium oxide, Cr_2O_3. Chromium(VI) compounds were potassium chromate, K_2CrO_4, and potassium dichromate, $K_2(Cr_2O_7)$. Solutions in molar ratios of 0.25 and 0.5 of Cr(VI)/total Cr [Cr(VI) from K_2CrO_4 and Cr(III) from $Cr(C_2H_3O_2)_3 \cdot H_2O$)] were also prepared for the infrared spectral calibration purposes. All aqueous solutions of chromate, dichromate, and chromium acetate hydrate of different concentrations were prepared at pH 7.4 (physiologic pH) in buffer solutions.

Model Minerals

Magnetite samples were obtained commercially from Minerals Unlimited (Ridgecrest, CA). Thin magnetite specimens were prepared by cleaving fragments off micro-fissiles. The specimen surfaces were cleaned by sonification in deionized and organic-free water for 15 min and sterilized by UV-irradiation for 20 min before use.

Sample Collection, Handling, and Preparation

The geologic samples were vesicular basalt cores (8.6 cm diameter) collected at a depth of 66–70 m at a site within the extensive Columbia basalt flow in southeastern Idaho (Figure 1). This site has been polluted with mixtures of hexavalent chromium, Cr(VI), and other inorganic ions, radionuclides, petroleum hydrocarbons, and volatile organic compounds (VOCs) from >40 years of U. S. nuclear production activity. The sampling technique, sample handling, and sectioning at the drilling site were conducted according to the protocol specifically developed to minimize disturbances to intrinsic microbial communities in the sample (Griffin et al. 1997).

Sectioned cores were transferred at the site into Whirl-pak bags and placed in sterile, argon-filled canisters, sealed, and shipped under Blue Ice by overnight express to our laboratory. Upon arrival, the cores were opened aseptically inside a sterile laminar hood to avoid

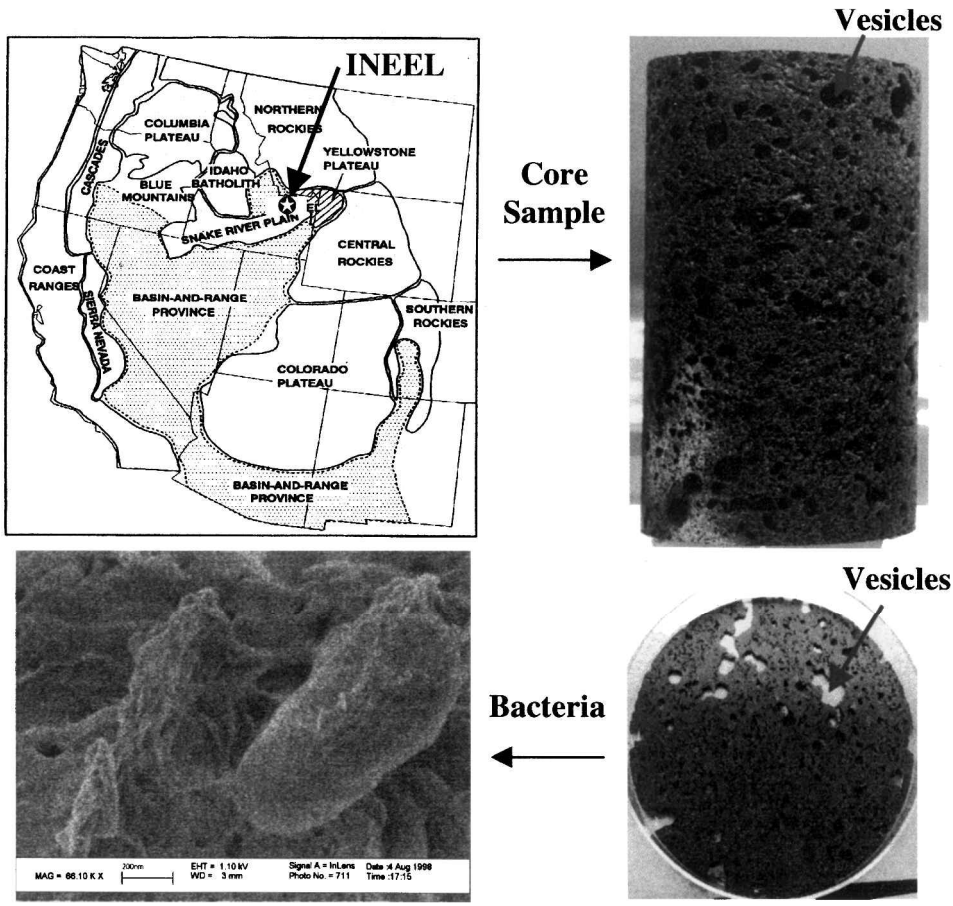

FIGURE 1 (Upper left) Map showing regional hydrogeologic provinces. The study area, formed from sequences of basalt flows, is within the Eastern Snake River Plain. Sampling location ✪ is inside US Department of Energy's Idaho National Engineering and Environmental Laboratory (INEEL). (Upper right) 8.6-cm-diameter basalt core samples were collected from 75 m below the ground surface but above the rock aquifer. The sample is fine-grained and covered with empty, gas-bubble cavities called vesicles. (Lower right) Section slice of core. (Lower left) SEM image of one of many bacteria types from the core sample.

contamination of samples for future microscopic and microbiologic analysis. Specimens 40- to 100-μm thick were prepared inside the hood by cleaving basalt fragments off the micro-fissile near the center of the rock samples. The center of the rock sample was assumed to be unlikely to suffer any ex situ bacterial contamination from the sample collection and handling processes. The specimens were stored aseptically at 4°C until used.

Sample Characterization

The Columbia basalt samples at the study site are fine-grained silicate-containing rocks, with calcicplagioclase feldspar [$(Na,Ca)(AlSi)_4O_4$], pyroxene [$(Ca,Na,Mg,Fe)(Al,Si)O_3$], and olivine ($Mg_{1.8}Fe_{0.2}SiO_4$) being the essential minerals (Sorenson et al. 1996). Magnetite ($Fe^{2+}Fe^{3+}{}_2)O_4$ is often also present. About 10–25% of the matrix consists of vesicles of

various sizes. Some vesicles are partly filled with individual or mixtures of minerals. Clusters of endoliths are present on the vesicles or on the fractured surfaces (Holman et al. 1998) although the Columbia basalt rock samples are generally quite limited in organic carbon. In areas where magnetite dominates, endoliths are often prolific. Confocal fluorescence micrographs of vertical sections show the thickness of the endolithic cluster to be generally $< 1\ \mu$m.

Identification of Cultivable Cr(VI)-Tolerant and -Reducing Endolithic Bacteria

Intrinsic endolithic bacteria were isolated and cultivated from the Columbia basalt samples by using the basalt rock extract agar described in Holman et al. (1998). The most Cr(VI)-tolerant endolithic bacteria were isolated by their growth on basalt rock extract agar that had been enriched with 100 mg/L chromate (as chromium). They were identified as Gram-positive *Arthrobacter oxydans* by fatty acid methyl ester (FAME) analysis (final identification of the isolate will be presented elsewhere). Extremely Cr(VI)-resistant *Arthrobacter* spp. strains have also been reported from other geographic areas (Margesin and Schinner 1996).

To test whether the Cr(VI)-tolerant *Arthrobacter oxydans* in Columbia basalt samples could also aerobically reduce Cr(VI), duplicate batch experiments were conducted inside 250-mL Erlenmeyer flasks containing 25 mL of basalt rock extract liquid medium enriched with 50 mg/L chromate. Control (abiotic) experiments were conducted in parallel with a similar medium but without the inoculation of *Arthrobacter oxydans*. To test the effect of concomitant biodegradation of organic co-contaminants on the reduction of Cr(VI), we added aliquots of dissolved toluene to the medium to produce a final aqueous toluene concentration of 5 ppm. After 2 weeks the concentration of Cr(VI) in the media was determined spectrophotometrically at μg/mL by diphenylcarbazide (American Public Health Association 1992). The amount of Cr(VI) reduction was 1.0–1.5% for the abiotic experiment, 3.9–4.5% for biotic, and 7.2% for biotic in the presence of dissolved toluene. *A. oxydans* can aerobically reduce Cr(VI) at a faster pace during concomitant biodegradation of volatile organic compounds such as toluene. Other bacteria with similar abilities to detoxify mixtures of Cr(VI) and organic compounds have been reported elsewhere (Shen et al. 1996).

SR-FTIR Spectromicroscopy Experiments of Surface Biogeochemical Reduction of Cr(VI)

Experiments of the biogeochemical reduction of Cr(VI) to Cr(III) were carried out on surfaces of model mineral phase magnetite and on surfaces of Columbia basalt samples. The experiment on magnetite surfaces was conducted abiotically (at the chromium/magnetite interfaces) and biotically (at the chromium/endolith/magnetite interfaces). The abiotic experiment used UV-sterilized and cleaved surfaces of magnetite without the introduction of intrinsic Cr(VI)-reducers *A. oxydans*.

The biotic experiment used UV-sterilized magnetite surfaces with the introduction of the resting cells of *A. oxydans*. Resting cells of *A. oxydans* were selected because the bacteria in geologic materials are "pre-grown." The cells were prepared from the stationary-phase living cells of *A. oxydans* by reculturing the purified *A. oxydans* in 100 mL of sterile basalt rock extract inside 1000-mL flasks. The purified cells were incubated at room temperature, and their growth was monitored by using a Hawksley counting chamber. The incubation continued with continuous stirring at 250 rpm until the growth reached its stationary-phase ($\sim$2 days). Cells were concentrated and cleaned by centrifugation at 5,000*g* for 10 min and washed with and resuspended in 10 mL of mineral salt medium three times. A 10-μl

portion of cell suspension (3×10^8 cells/mL) was introduced individually onto the magnetite surfaces, and solvent water was allowed to evaporate between introductions.

Biogeochemical reduction of Cr(VI) to Cr(III) on magnetite surfaces was also probed during concomitant biodegradation of toluene vapor. In this case the sterilized magnetite samples were exposed to 80 μL/L ppm toluene vapor at room temperature for 5 h (for sorption purposes) prior to the introduction of *A. oxydans*.

The experiment on magnetite surfaces began with a serial introduction of five 10-μL aliquots of 10 μg/L (as chromium) chromate solution onto surfaces of individual magnetite specimens. Five introductions were needed to produce sufficient infrared (IR) signals (at the location of observation) throughout the experimental study. Solvent water was allowed to evaporate between individual introductions. Localized high concentrations of chromium were observed because of the heterogeneous morphology of the surface.

All magnetite specimens were incubated in an aerobic atmosphere with 100% relative humidity inside 250-mL gas-tight I-CHEM Septa Jars (Fisher Scientific, USA) at room temperature (21 ± 1°C) in the dark. Real-time SR-FTIR spectra for the magnetite experimental system were recorded shortly after the start of the experiment and at the similar location 5 days after the exposure. Spatial distributions of vibrational frequencies associated with intrinsic microorganisms, chromate, toluene, and possible transformed chromium compounds were also mapped after the 5-day exposure.

The experiment of biogeochemical reduction of Cr(VI) on surfaces of Columbia basalt samples was conducted for 4 months. The experiment began with the sequential injection of 10 μL of chromate solution onto mineral surfaces in a basalt sample. To minimize the shock of chromate on intrinsic microorganisms, the chromate solution concentration in the injection fluid was gradually increased over a 4-day period: 10, 20, 30, and finally, 50 μg/L (as chromium). Individual basalt samples were incubated in the same aerobic atmosphere with 100% relative humidity inside 250-mL gas-tight Septa Jars at room temperature (21 ± 1°C) in the dark. The concentration of toluene vapor was maintained between 80 and 100 μL/L ppm throughout the experiment. Spatial distributions of vibrational frequencies associated with intrinsic microorganisms, chromate, and possibly reduced chromium compounds were mapped at the end of the second week and the end of the fourth month.

SR-FTIR Spectromicroscopy

The infrared spectromicroscopy facility on Beamline 1.4.3 at the Advanced Light Source, Lawrence Berkeley National Laboratory, was used to monitor the progress of Cr(VI) reduction at the Cr/endolith and Cr/mineral interfaces in both experiments. Figure 2 depicts the experimental setup for this direct measurement. As shown in the diagram, the infrared microprobe uses a synchrotron source that has much higher brightness than a conventional thermal IR source. The synchrotron light is incident onto a Nicolet Magna 760 FTIR bench, then is passed through a Nic-Plan IR microscope. As detailed elsewhere (Martin and McKinney 1998), the spot size of the unmasked synchrotron beam focused through the infrared microscope is ≤ 10 μm, nearly diffraction-limited, and significantly smaller than the 100 μm spot size attainable with similar strengths when using a conventional thermal IR source. This leads to an improved signal-to-noise ratio and finer spatial resolution than is possible for conventional source FTIR spectromicroscopy, thus enabling study of biogeochemical phenomena on surfaces of geologic materials that inherently are heterogeneous and have low IR reflectivity. The synchrotron IR beamline has an incident synchrotron IR energy range of 0.05 to 1.0 eV, which is nondestructive to biologic materials. This makes SR-FTIR spectromicroscopy extremely useful for detecting subtle biogeochemical changes as the Cr(VI) metal ions are exposed to endoliths, minerals, and various environmental chemicals.

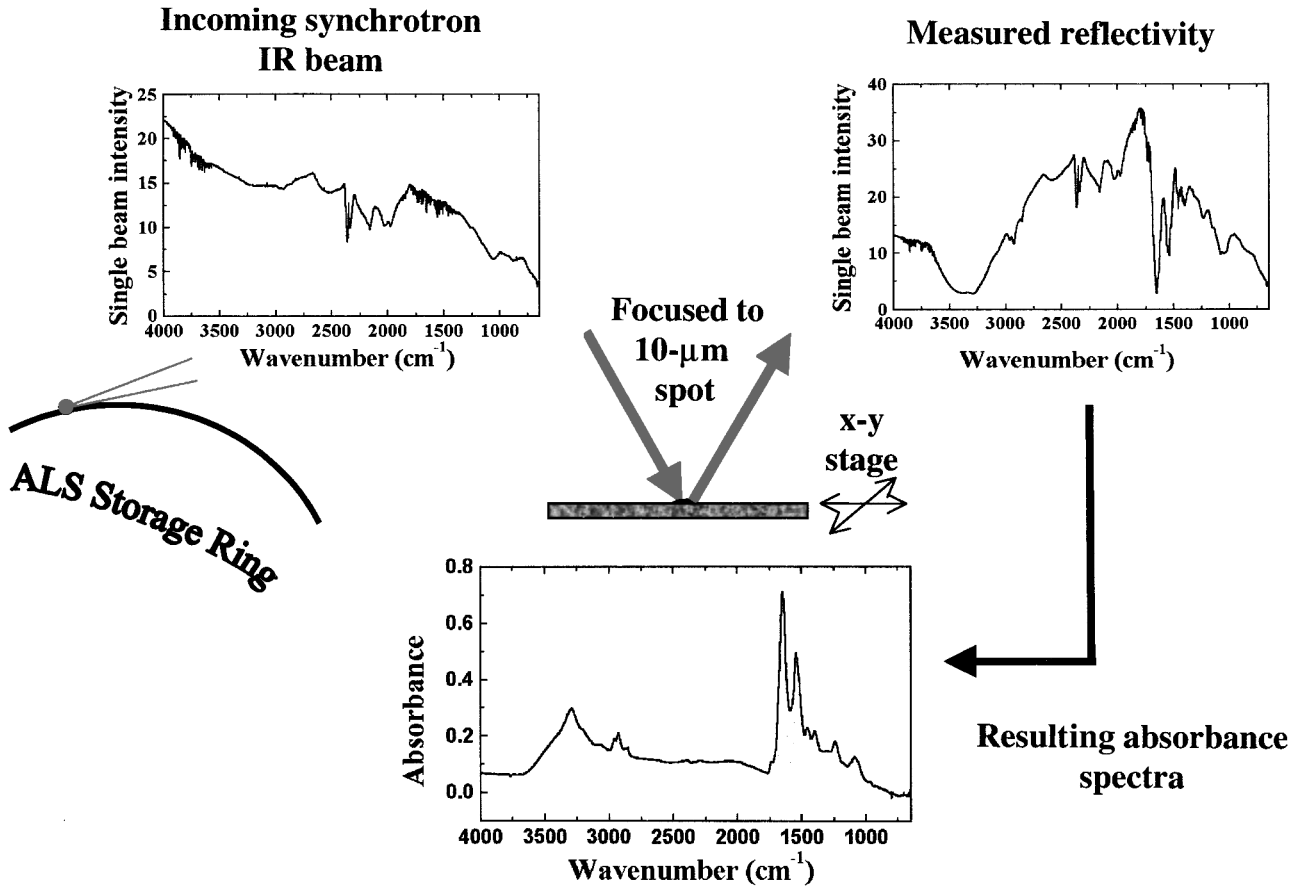

FIGURE 2 Diagram illustrating the experimental setup for measuring SR-FTIR spectra on sample surfaces. Note that the sample is placed on the microscope stage.

All SR-FTIR spectra were recorded in the 4000–650 cm^{-1} infrared region. This region was selected because it is the region that contains unique molecular fingerprint–exhibiting vibrational frequencies of functional groups of intact biomolecules (Brandenburg and Seydel 1996; Naumann et al. 1996), of chromium compounds of different oxidation states (Fujita et al. 1962a, b; Muller et al. 1969; Nakamoto 1986; Chertihin et al. 1997), and of toluene and its biodegradation products (Pouchert 1985; Greaves and Griffith 1991). For each IR measurement, 128 spectra were co-added at a spectral resolution of 4 cm^{-1}. All spectra were obtained in the reflectance (double-pass transmission) geometry and were ratioed to the spectrum of a bare gold-coated slide to produce absorbance values (see Figure 2). Any residual water vapor features in the resulting spectrum were removed by subtracting an appropriately scaled reference spectrum of water vapor.

The validity of SR-FTIR absorption spectra for endoliths, chromium compounds, toluene, and their possible transformation products was evaluated before its application to probing the spatial distribution and progress of surface biogeochemical reduction of Cr(VI) in the two experiments described above. The validation involved obtaining SR-FTIR spectra in the appropriate diagnostic spectral regions for thin films of endoliths and reference chemicals on gold-coated and on mineral surfaces. For reference chemicals that were unstable, all sample preparation and spectral measurements were conducted in an argon atmosphere. The relevant spectral characteristics of the recorded spectra were compared with those in the well-documented spectral research literature. Because the identity of the intermediate chromium compound(s) was unknown at the time of the validation study, only the SR-FTIR spectra for commercially available chromium oxides of different oxidation states were recorded, and the signals of Cr-O vibrations were compared.

At the end of the SR-FTIR spectromicroscopy study, the measured spatial distribution of elemental chromium on surfaces of Columbia basalt samples and the chromium oxidation state were verified by using micro-x-ray spectroscopy techniques.

μ-XRF and μ-XAFS Spectromicroscopy

The micro-x-ray facility on Beamline 10.3.2 at the Advanced Light Source was used to validate the final results from the SR-FTIR spectromicroscopy study. This beamline currently has a spatial resolution of 0.8 μm and an incident x-ray energy range of 4–14.0 keV (MacDowell et al. 1998), which is orders of magnitude more intense than the IR beam. To our knowledge, the only stable oxidation states under normal ambient conditions and thus observable with XAFS are Cr(VI), Cr(III), and Cr(0). The oxidation state of Cr(V) is stable only in living biologic systems (e.g., Suzuki et al. 1992; Cooke et al. 1995, Itoh et al. 1995). Because the intense high energy of the x-ray beam (in contrast to the synchrotron IR beam) can kill living microorganisms, Cr(V) without the presence of living microorganisms is not stable long enough under normal ambient conditions to be observable with XAFS.

The basalt sample was mounted in an x-ray–transparent holder and was positioned at 45° to both the incoming beam and the SiLi detector. All measurements were taken over the approximate area studied during the SR-FTIR spectromicroscopy experiment. The spatial distribution of elemental chromium on surfaces of the sample was evaluated by μ-XRF spectroscopy. This technique measures the characteristic fluorescence yield for a given element. Because the beam size is on the order of 1 μm, it provides an accurate means of determining the chromium spatial distribution.

The oxidation state of the detected chromium was determined by μ-XAFS spectroscopy. The Cr(III) model compound used for μ-XAFS spectral calibration was chromium hydroxide, γ-CrOOH. The Cr(VI) model compound was potassium chromate, K_2CrO_4. For the K-edges shifts for the first-row transition metals, a typical value was 1–3 eV per change

in oxidation state (Wong et al. 1984; Bajt et al. 1993; Sutton et al. 1993). Differentiating between Cr(VI) and Cr(III) is particularly easy because Cr(VI) also exhibits a large pre-edge peak a few electrovolts before the edge, which does not exist for Cr(III).

Results

SR-FTIR Spectromicroscopy Validation and Analysis

Table 1 summarizes the appropriate diagnostic spectral regions and the distinct SR-FTIR absorption bands within each region that would be used in the remaining study as chemical molecule markers to elucidate the Cr(VI) reduction process. The global spectral features of *A. oxydans* and mixtures of endoliths recorded by SR-FTIR spectromicroscopy on gold-coated surfaces and surfaces of magnetite and basalt were consistent with those reported in the literature (Brandenburg and Seydel 1996; Naumann et al. 1996). All had well-documented prominent SR-FTIR absorption envelopes arising from the C= O functional group of biomolecules: the stretching vibrations in the 1695–1620 cm^{-1} region of protein amide I with C= O weakly coupled to the N–H stretching mode, and the bending vibrations in the 1570–1515 cm^{-1} region of protein amide II with C= O strongly coupled to the N–H stretching mode. Gram-negative isolates exhibited an additional but relatively weak ester carbonyl peak near 1741 cm^{-1}, which arises from the C= O ester stretching vibration of phospholipids in their additional outer membrane.

The recorded SR-FTIR spectral features of potassium chromate are distinguished by a strong band near 846 cm^{-1} and a weaker band near 890 cm^{-1}, which agree with those reported for Cr–O vibration of $(CrO_4)^{2-}$ in the literature (Campbell 1965; Nakamoto 1986). The recorded spectral features of Cr(III) acetate hydrate have a strong absorption band near 810 cm^{-1} and a weaker band near 798 cm^{-1}, which agree with those reported for Cr–O vibration of $[Cr(OH)_3]^{3-}$ in the literature (Fujita et al. 1962a). Because Cr(V) compounds are not available commercially, absorption bands near 836 cm^{-1} and 765 cm^{-1}, reported in the literature for Cr–O vibration of $(CrO_4)^{3-}$ (Nakamoto 1986), were used to guide the interpretation of our recorded SR-FTIR spectra.

The recorded global spectral features of toluene and its early biodegradation product catechol are consistent with those reported in the literature (Pouchert 1985; Greaves and Griffith 1991). Within the diagnostic region, toluene has a strong marker absorption band near 728 cm^{-1} and a weaker band near 695 cm^{-1}. For catechol, the marker absorption bands are 770 cm^{-1} and 742 cm^{-1}.

TABLE 1 Spectral regions and distinct absorption bands within each region for endoliths (including bacteria), Cr(VI)-, Cr(V)-, and Cr(III)-compounds, toluene, and catechols

Compounds	Spectral regions (cm^{-1})	Absorption bands (cm^{-1})
Endoliths	1800–1500	~1650; ~1550
Cr(VI)-compounds	900–800	~846; ~890
Cr(V)-compounds	900–700	~830; ~764
Cr(III)-compounds	850–750	~810; ~798
Toluene	800–650	~728; ~695
Catechols	800–700	~770; ~742

SR-FTIR Spectromicroscopy of Cr(VI) Reduction on Magnetite Surfaces

Figure 3 shows the recorded SR-FTIR spectra for chromate on magnetite surfaces shortly after the experiment's beginning and 5 days after exposure. For magnetite surfaces without living *A. oxydans* cells (abiotic), there were no statistically significant changes in either the IR absorption intensity or the characteristic band shapes within the diagnostic spectral region of chromium during the 5-day period.

For magnetite surfaces with living *A. oxydans* cells (biotic), the noticeable changes were the moderate decrease in the absorption intensity of the chromate $(CrO_4)^{2-}$ vibrational mode at 846 cm^{-1}. Meanwhile, a weaker band at 830 cm^{-1} appeared and was accompanied by an even weaker one at 765 cm^{-1}. These bands are reminiscent of the reduced transition metal ions of Cr(V) the IR-active stretching frequencies of Cr–O in chromium–carboxylate and chromium–amino acid complexes (Nakamoto 1986), and the vibrations of the oxalate (Fujita et al. 1962a) and catecholate (Griffith et al. 1986) anions that can both complex with transition metal ions of Cr(V). The existence of Cr(V) compounds as an intermediate product of the microbial reduction of Cr(VI) to Cr(III) has been reported (Suzuki et al. 1992; Cooke et al. 1995; Itoh et al. 1995). Furthermore, all of these organic classes of compounds listed above have been documented as being natural products of microbial activities (Johnston and Vestal 1993; Russell et al. 1998), although it is virtually impossible to establish precisely which Cr(V) complexes are being observed (Faulques et al. 1998). Aerobic Cr(VI) reduction observed here is generally believed to be caused by "enzymatic" or "indirect" processes. An enzymatic process implies that the Cr(VI) reduction is tied to enzymes that are produced intracellularly by biologic processes, including respiration. An "indirect" process implies that Cr(VI) is reduced in the extracellular medium by inorganic and organic reductants, which are themselves produced by biologic processes. To date, it is not yet understood if our observed aerobic reduction reaction took place intracellularly or extracellularly, or both. Research activity is now underway to address this issue.

For magnetite surfaces with both the living *A. oxydans* cells and the concomitant biodegradation of toluene, all infrared absorption bands in the diagnostic spectral regions displayed significant changes in both intensity and characteristic band shape for the 5-day experiment (Figure 3). In particular, the absorption intensities of the 846 cm^{-1} and 728 cm^{-1} modes, which are assigned to $(CrO_4)^{2-}$ and toluene, respectively, disappeared. At the same time, a new, strong band at 830 cm^{-1} appeared and was accompanied by a sharp but weaker satellite at 765 cm^{-1}, which was again associated with a possible intermediate Cr(V) species. The additional new band at 742 cm^{-1}, accompanied by a sharp and slightly weaker satellite at 770 cm^{-1}, is possibly associated with catechol, one of toluene's many documented biodegradation products (Cerniglia 1984). The cause of this accelerated aerobic reduction reaction is not certain but may arise from the increasing microbial activity, which is further enhanced by an array of reactive organic molecules produced during concomitant biodegradation of toluene. For example, catechol, a byproduct of microbial degradation of toluene, can by itself reduce Cr(VI) (Deng and Stone 1996).

The spatial distributions of the IR absorption associated with protein amide II of *A. oxydans* (1550 cm^{-1}), a 5-day exposure to chromate (846 cm^{-1}), and toluene (728 cm^{-1}), as discussed in the preceding paragraph, were mapped and are presented in Figure 4. Multiple variable regression analysis shows a spatial correlation coefficient (r^2) of 0.86 ± 0.03 for the three measured values displayed in the three maps. This reveals the close link between the microbial reduction of Cr(VI) and the biodegradation of toluene. It also reveals that the transformation of chromate and toluene during the 5-day experimental period was controlled spatially by the microorganism distribution on magnetite surfaces. The spectral characteristics recorded at the maximum chromate depletion location were similar to those

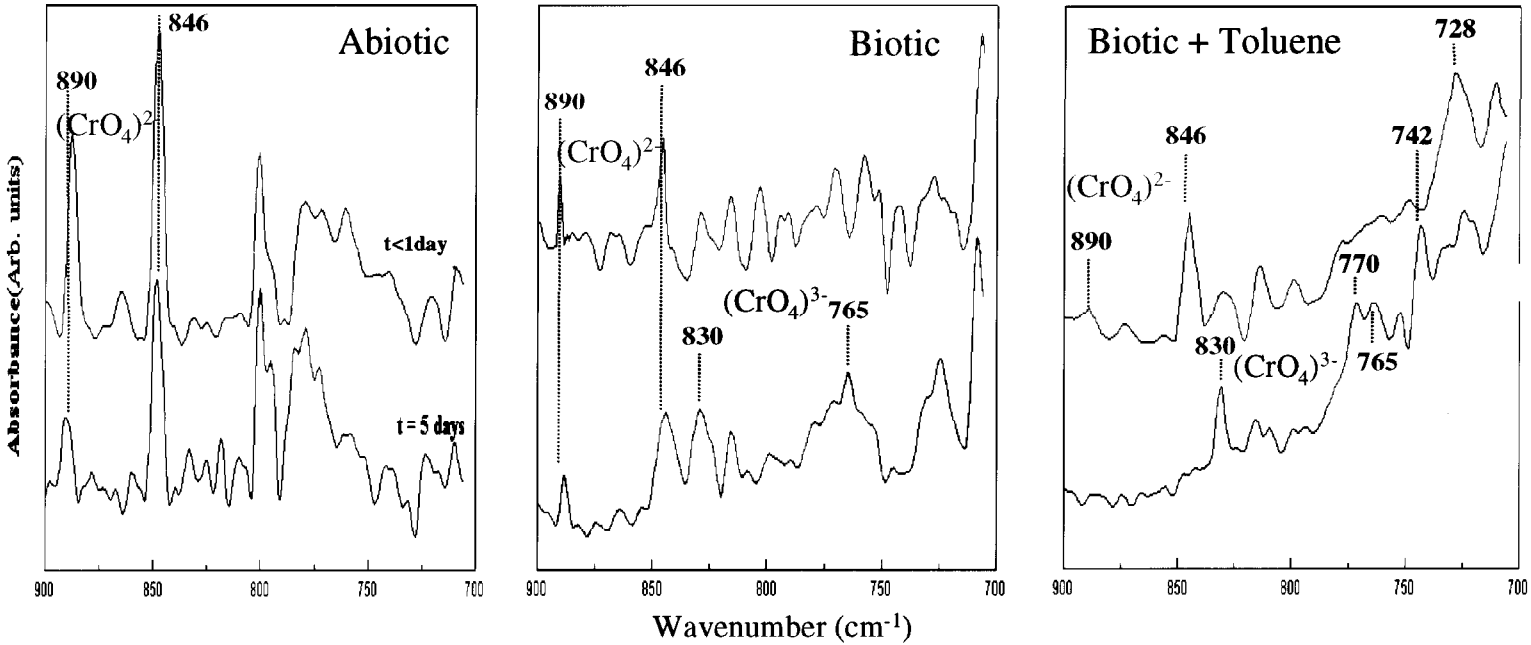

FIGURE 3 SR-FTIR spectra of chromate on magnetite surfaces during the 5-day experiment of (left) abiotic reduction, (middle) biotic reduction in the absence of other organic compounds, and (right) biotic reduction in the presence of toluene vapor (as a model volatile organic compound). ——— t < 1 day, shifted vertically for visual clarity. ——— t = 5 days. Although the total chromate $(CrO_4)^{2-}$ concentration for each of the three experiments were the same, microbial–mineral surface roughness and redistribution during evaporation resulted in heterogeneous spatial distributions of $(CrO_4)^{2-}$ concentrations. The most relevant vibrational frequencies identified are marked: 890 and 846 cm^{-1} correspond to $(CrO_4)^{2-}$ (green), 830 and 765 cm^{-1} correspond to $(CrO_4)^{3-}$ (blue), 770 and 742 cm^{-1} are catechols, and 728 cm^{-1} is toluene (red). Microbial reduction of Cr^{6+} was the dominant mechanism in our experimental system. The microbial chromium reduction was further enhanced during the microbial degradation of the organic compound toluene.

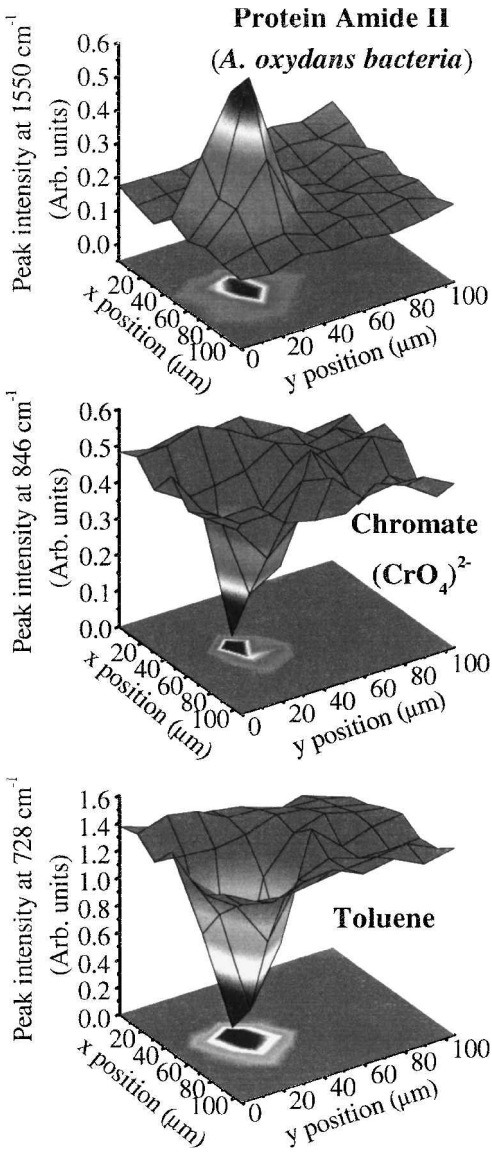

FIGURE 4 During the 5-day study period, *Arthrobacter oxydans* bacteria (isolated from the basalt core sample) attached themselves to magnetite surfaces. They reduced Cr(VI) while degrading toluene. SR-FTIR spectromicroscopy measurements at the end of the experiment show the spatial distribution of (top) *A. oxydans*, (middle) chromate, and (bottom) toluene, as measured by their spectral signatures.

in Figure 3 (right panel), which demonstrate that the decrease in the absorption intensity at the Cr(VI) vibrational frequency 846 cm^{-1} is probably caused by chromium transformation to the possible intermediate products of Cr(V) compounds such as $(CrO_4)^{3-}$ or a complex of organic molecules with Cr(III), as described above. The lack of significant chromate reduction on surfaces that are either free of, or low in, *A. oxydans* density implies that the microbial reduction mechanism is significant even on surfaces of mixed iron oxides.

SR-FTIR Spectromicroscopy of Cr(VI) Reduction on Columbia Basalt Surfaces

Two weeks after the chromate exposure, spectral mappings of endolith-occupied areas of Columbia basalt specimens revealed vibrational frequencies associated with the possible intermediate Cr(V) compounds but not with the possible Cr(III) compounds. The lack of vibrational frequencies associated with the presence of possible Cr(III) compounds across the sample surfaces implies that a 2-week duration is only long enough to reduce chromate to its possible intermediate Cr(V) compounds. It is not long enough to reduce Cr(VI) to the final Cr(III) state. In addition, the same spectral mapping reveals a widespread distribution of Cr(V) but an insignificant spatial relationship between the IR absorbance of the possible intermediate Cr(V) compounds and the endoliths. The multiple variable analysis shows a small spatial correlation coefficient ($r^2 < 0.01$). A one-way analysis of variance, which is used to account for the effect of composite minerals on the spatial relationship between the Cr(VI) reduction to Cr(V) and the distribution of microorganisms, is not significant ($p > 0.1$).

At the end of the fourth month, spatial distributions of the same vibrational frequencies 1550 cm^{-1} and 830 cm^{-1} are shown in Figure 5. The overall spatial distribution demonstrated an improved correlation between the Cr(VI) reduction to Cr(III) and the distribution of endoliths. Although the multiple variable analysis still shows an insignificant spatial correlation coefficient ($r^2 < 0.01$) for the two measured values, the one-way analysis of variance is significant ($p < 0.03$). This implies that a 4-month incubation time has selectively enriched successful growth of chromate-tolerant and -reducing native endoliths. Spectral characteristics of typical SR-FTIR spectra recorded at locations outside the maximum Cr(III) location exhibited stretching frequencies typical of Cr(V) compounds as discussed earlier. Very little Cr(VI) was detected.

μ-XRF and μ-XAFS Spectromicroscopy Results

Figure 6 shows the spatial distribution of elemental chromium on the surfaces of Columbia basalt samples as measured by μ-XRF spectroscopy. This spatial pattern is similar to the spatial distribution of Cr(III) compounds measured by SR-FTIR spectromicroscopy (see Figure 5). Peak μ-XAFS intensity data recorded at the similar location as the peak IR absorption intensity for Cr(III) compounds (in Figure 5) show a Cr x-ray absorption edge structure feature and at the same time a lack of pre-edge peak (Figure 6a). The lack of pre-edge peak is consistent with both the μ-XAFS pre-edge feature of our Cr(III) model compound described earlier and those reported in the literature (e.g., Wong et al. 1984; Sutton et al. 1993; Peterson et al. 1997). This result shows that the Cr(VI) had indeed been reduced to Cr(III) under the conditions of the experiments described in this paper. The SR-FTIR and the XAFS experiments were repeated after 3 months and continued to indicate no reoxidation of Cr(III). This implies that the reduced Cr(III) is relatively stable under normal atmospheric conditions.

Conclusion

This study demonstrates for the first time that SR-FTIR spectromicroscopy is a promising tool to complement existing techniques for nondestructively monitoring the progress and elucidating the dominant mechanisms and possible pathways of IR-amenable chemicals on mineral surfaces. Within our chromium/endolith/mineral system, we have demonstrated in real-time that the microbial reduction of Cr(VI) in an aerobic environment is important even in the presence of mixed mineral oxides. Time-resolved studies indicate that the microbial reduction of Cr(VI) to Cr(III) proceeds at least as a two-step reaction, possibly

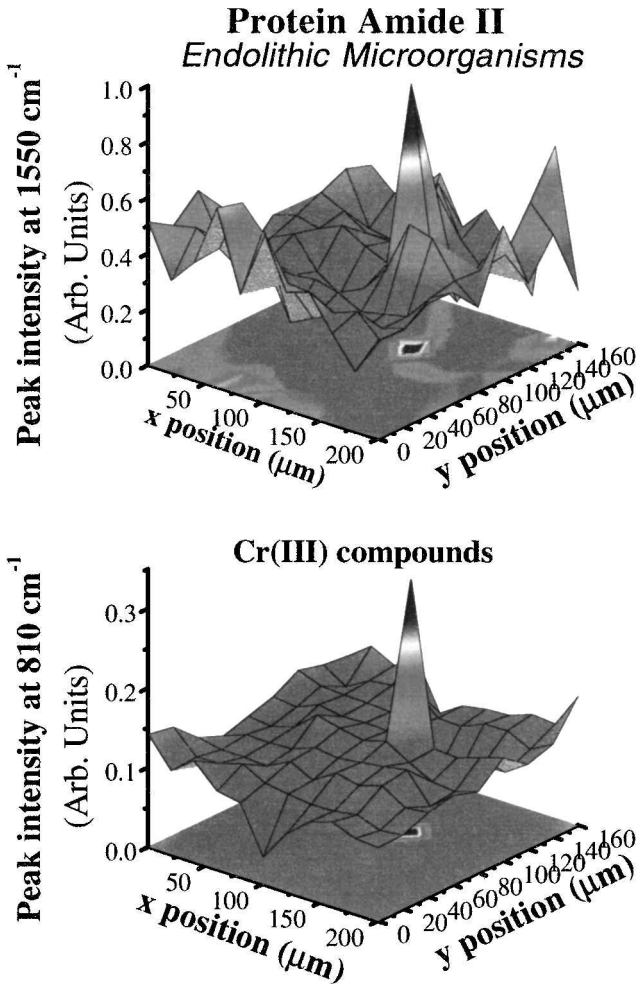

FIGURE 5 Distribution of indigenous endolithic microorganisms (top) and the Cr(III) compounds (bottom) as measured by SR-FTIR spectromicroscopy at the end of the 4-month Cr(VI)–microbe–basalt experiment. Only chromium-tolerant and chromium-reducing microorganisms proliferated during the study period.

with Cr(V) compounds as intermediate products. In addition, the Cr(VI) reduction reaction accelerates during the concomitant biodegradation of toluene (a common co-contaminant), which further confirms the significance of the biologic activities. The spatially resolved SR-FTIR spectromicroscopy shows that on magnetite and basalt surfaces, Cr(VI) is reduced only in the presence of endoliths. The reduction-produced Cr(III) compounds observed were confirmed by μ-XAFS spectroscopy. The reduced chromium compounds appear to be stable for many months in an aerobic environment, implying that the mutagenic Cr(VI) pollutants in the environment can be biotransformed aerobically into less mobile, less toxic, and more stable compounds. With this effort, the potential use of SR-FTIR spectromicroscopy for providing mechanistic information on the reduction of Cr(VI) has been demonstrated.

The SR-FTIR spectromicroscopy technique is limited to the study of microbial/chemical contaminant systems with interpretable infrared spectral fingerprints and a spatial resolution of ~ 10 μm or larger. Another intrinsic limitation of the technique in geologic samples

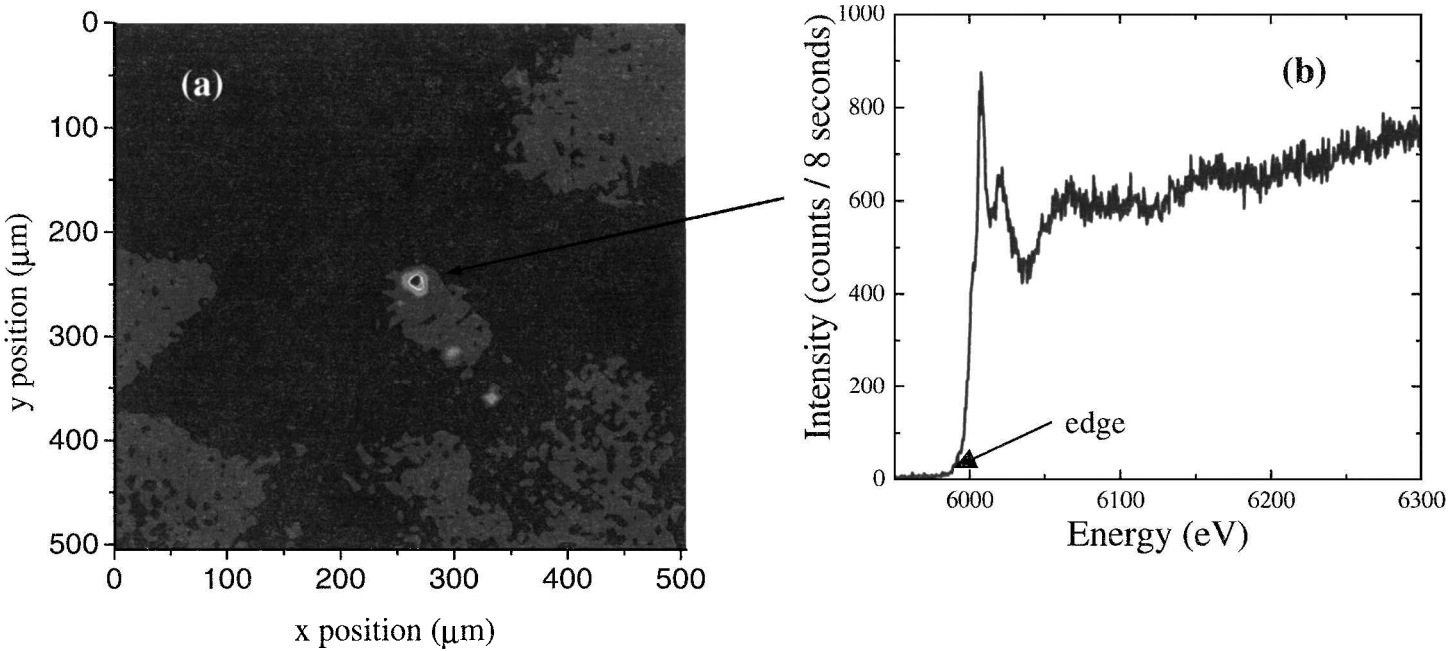

FIGURE 6 Confirmation of chromium (III) oxidation state by micro-x-ray analysis on the similar area of the identical sample studied by SR-FTIR (see Figure 5). (a) Chromium elemental mapping by μ-XRF analysis. The colors go from black (chromium concentration below detection limit) to red (high chromium concentration). (b) μ-XAFS scan at the highest concentration spot shows no Cr(VI) pre-edge peak and is consistent with Cr(III) compounds.

is that the spectral information obtained is qualitative. It is difficult from a practical standpoint to obtain absolute quantitative information because of the heterogeneous nature and the roughness of the surfaces of geologic materials. Also, a complete understanding and assignment of all bands in the infrared spectra of the combined biological, chemical, and mineral systems is extremely difficult, given the complexity of the samples. Despite these technical difficulties, we have been able to identify IR signals that enable us to follow the key mechanisms and possible pathway of Cr(VI) reduction to Cr(III) on basalt surfaces.

References

Ahmann D. 1997. Bioremediation of metal-contaminated soil. Soc Ind Microbiol 47:218–233.

American Public Health Association. 1992. 3500-Cr D. Colorimetric method. In: Standard methods for the examination of water and wastewater, 18th ed. Baltimore: Victor Graphic, p 3.59–3.60.

Bajt S, Clark SB, Sutton SR, Rivers ML, Smith JV. 1993. Synchrotron x-ray microprobe determination of chromate content using x-ray absorption near edge structure. Anal Chem 65:1800–1804.

Bantignies JL, Cartier C, Dexpert H, Flank AM, Williams GP. 1995. Ashpaltene adsorption on kaolinite—characterization by infrared microspectroscopy and x-ray absorption spectroscopy. C R Acad Sci 320:699–706.

Bidoglio G, Gibson PN, O'gorman M, Roberts KJ. 1993. X-ray absorption spectroscopy investigation of surface redox transformations of thallium and chromium on colloidal mineral oxides. Geochim Cosmochim Acta 57:2389–2394.

Biino GG, Mannella N, Kay A, Mun B, Fadley CS. 1998. Surface chemical characterization and surface diffraction effects of real margarite(001): an angle-resolved XPS investigation (X-ray photoelectron spectroscopy). Am Mineral 84:629–638.

Brandenburg K, Seydel U. 1996. Fourier-transform infrared spectroscopy of cell surface polysaccharides. In: HH Henry, D Chapman, editors. Infrared spectroscopy of biomolecules. New York: Wiley-Liss, p 203–238.

Campbell JA. 1965. Spectral evidence for interionic forces in crystals—chromates and dichromates. Spectrochim Acta 21:1333–1343.

Cerniglia CE. 1984. Microbial transformation of aromatic hydrocarbons. In: RM Atlas, editor. Petroleum microbiology. New York: Macmillan, p 99–128

Cheah S-F, Brown GE Jr, Parks GA. 1998. XAFS spectroscopy study of Cu(II) sorption on amorphous SiO_2 and γ-Al_2O_3: effect of substrate and time on sorption complexes. J Colloid Interface Sci 208:110–128.

Chertihin GV, Bare WD, Andrews L. 1997. Reactions of laser-ablated chromium atoms with dioxygen. Infrared spectra of CrO, OCrO, CrOO, CrO_3, $Cr(OO)_2$, Cr_2O_2, Cr_2O_3 and Cr_2O_4 in solid argon. J Chem Phys 107:2798–2806.

Conradson SD. 1998. Application of x-ray absorption fine structure spectroscopy to materials and environmental science. Appl Spectrosc 52:252A–279A.

Cooke VM, Hughes MN, Poole RK. 1995. Reduction of chromate by bacteria isolated from the cooling water of an electricity generating station. J Ind Microbiol 14:323–328.

Deng BL, Stone AT. 1996. Surface-catalyzed chromium(VI) reduction—reactivity comparisons of different organic reductants and different oxide surfaces. Environ Sci Technol 30:2484–2494.

Ehrlich HL. 1990. Geomicrobiology. New York: Marcel Dekker, p 441–448.

Faulques E, Perry DL, Lott S, Zubkowski JD, Valente EJ. 1998. Study of coordination and ligand structure in cobalt–EDTA complexes with vibrational microspectroscopy. Spectrochim Acta 54:869–878.

Fiedor JN, Bostick WD, Jarabeck RJ, Farrell J. 1998. Understanding the mechanism of uranium removal from groundwater by zero-valent iron using x-ray photoelectron spectroscopy. Environ Sci Technol 32:1466–1473.

Fujita J, Martell AE, Nakamoto K. 1962a. Infrared spectra of metal chelate compounds. VI. A normal coordinate treatment of oxalato metal complexes. J Chem Phys 36:324–331.

Fujita J, Martell AE, Nakamoto K. 1962b. Infrared spectra of metal chelate compounds. VII. Normal coordinate treatments on 1:2 and 1:3 oxalato complexes. J Chem Phys 36:331–338.

Greaves SJ, Griffith WP. 1991. Vibrational spectra of catechol, catechol-d2 and -d6 and the catecholate monoanion. Spectrochim Acta 47A:133–140.

Griffin WT, Phelps TJ, Colwell FS, Fredrickson JK. 1997. Methods for obtaining deep subsurface microbiological samples by drilling. In: PS Amy, DL Haldeman, editors. The microbiology of the terrestrial deep subsurface. New York: CRC Lewis Publishers, p 23–44.

Griffith WP, Pumphrey CA, Rainey T-A. 1986. Catecholato complexes of ruthenium, iridium, rhenium, molybdenum, and tungsten. J Chem Soc Dalton Trans 1125–1128.

Guilhaumou N, Dumas P, Carr GL, Williams GP. 1998. Synchrotron infrared microspectrometry applied to petrography in micrometer-scale range: fluid chemical analysis and mapping. Appl Spectrosc 52:1029–1034.

Guo TZ, DeLaune RD, Patrick WH. 1997. The influence of sediment redox chemistry on chemically active forms of arsenic, cadmium, chromium, and zinc in estuarine sediment. Environ Int 23:305–316.

Holman H-YN, Perry DL, Hunter-Cevera JC. 1998. Surface-enhanced infrared absorption-reflectance (SEIRA) microspectroscopy for bacteria localization on geologic material surfaces. J Microbiol Methods 34:59–71.

Itoh M, Nakamura M, Suzuki T, Kawai K, Horitsu H, Takamizawa K. 1995. Mechanism of chromium(VI) toxicity in *Escherichia coli*: is hydrogen peroxide essential in Cr(VI) toxicity? J Biochem 117:780–786.

Jamin N, Dumas P, Moncuit J, Fridman W-H, Teillaud JL, Carr GL, Williams GP. 1998. High resolved chemical imaging of living cells by using synchrotron infrared microspectrometry. Appl Biol Sci 95:4837–4840.

Johnston CG, Vestal JR. 1993. Biogeochemistry of oxalate in the Antarctic Cryptoendolithic lichen-dominated community. Microb Ecol 3:305–319.

Kaplan DI, Hunter DB, Bertsch PM, Bajt S, Adriano DC. 1994. Application of synchrotron x-ray fluorescence spectroscopy and energy dispersive x-ray analysis to identify contaminant metals on groundwater colloids. Environ Sci Technol 28:1186–1189.

Kostka JE, Nealson KH. 1995. Dissolution and reduction of magnetite by bacteria. Environ Sci Technol 29:2535–2540.

Losi ME, Amrhein C, Frankenberger WT Jr. 1994. Factors affecting chemical and biological reduction of hexavalent chromium in soil. Environ Toxicol Chem 13:1727–1735.

Lovley DR, Coates JD. 1997. Bioremediation of metal contamination. Curr Opin Biotechn 8:285–289.

MacDowell AA, Chang C-H, Lamble GM, Celestre RS, Padmore JR, Patel JR. 1998. Progress towards sub-micron hard x-ray imaging using elliptically bent mirrors and its applications. In: X-ray microfocusing: applications and techniques. Proc, Int Soc Optical Eng 3449:137–144.

Margesin R, Schinner F. 1996. Bacterial heavy metal-tolerance-extremeresistance to nickel in *Arthrobacter* spp. strains. J Basic Microbiol 36:269–282.

Martin CM, McKinney WR. 1998. The first synchrotron infrared beamlines at the Advanced Light Source: microspectroscopy and fast timing. In: SM Mini, SR Stock, DL Perry, LJ Terminello, editors. Applications of synchrotron radiation techniques to materials science IV. Materials Research Society Proc 524:11–16.

Muller O, White WB, Roy R. 1969. Infrared spectra of the chromates of magnesium, nickel and cadmium. Spectrochim Acta 25A:1491–1499.

Nakamoto K. 1986. Infrared and Raman spectra of inorganic and coordination compounds, 4th ed. New York: Wiley, 484 p.

Naumann D, Shultz CP, Helm D. 1996. What can infrared spectroscopy tell us about the structure and composition of intact bacterial cells? In: HH Henry, D Chapman, editors. Infrared spectroscopy of biomolecules. New York: Wiley-Liss, p 279–310.

Nieboer E, Jusys AA. 1988. Biologic chemistry of chromium. In: JO Nriagu, E Nieboer, editors. Chromium in the natural and human environments. New York: John Wiley & Sons, p 21–80.

Ohtake H, Silver S. 1994. Bacterial detoxification of toxic chromate. In: GR Chaudhry, editor. Biologic degradation and bioremediation of toxic chemicals. New York: Chapman & Hall, p 403–415.

Perry DL, Taylor JA, Wagner CD. 1990. X-ray-induced photoelectron and Auger spectroscopy. In: DL

Perry, editor. Instrumental surface analysis of geologic materials. New York: VCH Publishers Inc., p 45–86.

Peterson ML, Brown GE Jr, Parks GA, Stein CL. 1997. Differential redox and sorption of Cr(III/VI) on natural silicate and oxide minerals: EXAFS and XANES results. Geochim Cosmochim Acta 61:3399–3412.

Pouchert CJ. 1985. The Aldrich library of FT-IR spectra. Milwaukee, WI: Aldrich Chemical Co., Vol 1, p 931–970.

Russell NC, Edwards HGM, Willliams DD. 1998. FT-Raman spectroscopic analysis of endolithic microbial communities from Beacon sandstone in Victoria Land, Antarctica. Antarct Sci 10:63–74.

Shen H, Prithard PH, Sewell GW. 1996. Kinetics of chromate reduction during naphthalene degradation in a mixed culture. Biotechnol Bioeng 52:357–365.

Silver S. 1998. Genes for all metals—a bacterial view of the Periodic Table. J Ind Microbiol Biotechnol 20:1–12.

Snow ET. 1991. A possible role for chromium(III) in genotoxicity. Environ Health Perspect 92:75–81.

Sorenson KS, Wylie AH, Wood TR. 1996. Test Area North. Hydrogeologic studies test plan operable unit 1-07B. Lookheed Idaho Technologies Co., Idaho Falls, ID, INEL-96/0105, p 2–10.

Sutton SR, Jones KW, Gordon B, Rivers ML, Bajt S, Smith JV. 1993. Reduced chromium in olivine grains from lunar basalt 15555: x-ray absorption near edge structure (XANES). Geochim Cosmochim Acta 57:461–468.

Suzuki T, Miyata N, Horitsu H, Kawai K, Takamizawa K, Tai Y, Okazaki M. 1992. NAD(P)H-dependent chromium(VI) reductase of *Pseudomonas ambiqua* G-1: a Cr(V) intermediate is formed during the reduction of Cr(VI) to Cr(III). J Bacteriol 174:5340–5345.

Turick CE, Apel WA, Carmiol NS. 1996. Isolation of hexavalent chromium-reducing anaerobes from hexavalent-chromium-contaminated and non-contaminated environments. Appl Microbiol Biotechnol 44:683–688.

Wang Y-T, Shen H. 1995. Bacterial reduction of hexavalent chromium. J Ind Microbiol 14:159–163.

Wong J, Lytle FW, Messmer RP, Maylotte DH. 1984. *K*-edge absorption spectra of selected vanadium compounds. Phys Rev B30:5596–5610.

Wong PK, Fung KY. 1997. Removal and recovery of nickel ion (Ni^{2+}) from aqueous solution by magnetite-immobilized cells of *Enterobacter* sp. 4-2. Enzyme Microb Technol 20:116–121.